Muon g-2 and a type-X two Higgs doublet scenario: some studies in high-scale validity

Atri Dey

November 11,2021

Based on - arXiv:2106.01449

With **J. Lahiri, B. Mukhopadhyaya**
Harish-Chandra Research Institute, Allahabad

Table of Contents

Motivation

Motivation

- In today's context, the long-standing discrepancy between SM prediction and experimental observation on the anomalous magnetic moment of muon hints towards new physics.

Motivation

- In today's context, the long-standing discrepancy between SM prediction and experimental observation on the anomalous magnetic moment of muon hints towards new physics.
- The Type-X 2HDM can explain the observed muon anomaly with a very low mass pseudoscalar.

Motivation

- In today's context, the long-standing discrepancy between SM prediction and experimental observation on the anomalous magnetic moment of muon hints towards new physics.
- The Type-X 2HDM can explain the observed muon anomaly with a very low mass pseudoscalar.
- **problem:** The low pseudoscalar(A) mass region are highly constrainted from $h_{SM} \to AA$ searches($Br(h_{SM} \to AA) \leq 4\%$).

Motivation

- In today's context, the long-standing discrepancy between SM prediction and experimental observation on the anomalous magnetic moment of muon hints towards new physics.
- The Type-X 2HDM can explain the observed muon anomaly with a very low mass pseudoscalar.
- **problem:** The low pseudoscalar(A) mass region are highly constrainted from $h_{SM} \to AA$ searches($Br(h_{SM} \to AA) \leq 4\%$).
- **The question we ask here is:** can the aforesaid aspects of low-energy phenomenology provide any hint of the UV completion of this scenario?

Overview of the Model

- Most general scalar potential involving two scalar doublets, under the assumption of a softly broken discrete Z_2 symmetry,

$$\begin{aligned}\mathcal{V} &= m_{11}^2\Phi_1^\dagger\Phi_1 + m_{22}^2\Phi_2^\dagger\Phi_2 - [m_{12}^2\Phi_1^\dagger\Phi_2 + \mathrm{h.c.}] + \frac{1}{2}\lambda_1(\Phi_1^\dagger\Phi_1)^2 \\ &+ \frac{1}{2}\lambda_2(\Phi_2^\dagger\Phi_2)^2 + \lambda_3(\Phi_1^\dagger\Phi_1)(\Phi_2^\dagger\Phi_2) + \lambda_4(\Phi_1^\dagger\Phi_2)(\Phi_2^\dagger\Phi_1) \\ &+ \left\{\frac{1}{2}\lambda_5(\Phi_1^\dagger\Phi_2)^2 + \mathrm{h.c.}\right\}. \end{aligned} \tag{1}$$

- Two CP-even physical states defined as:

$$\begin{aligned} H &= (\phi_1^0)\cos\alpha + (\phi_2^0)\sin\alpha\,, \\ h &= -(\phi_1^0)\sin\alpha + (\phi_2^0)\cos\alpha\,, \end{aligned}$$

- CP-odd neutral scalar defined as A and a pair of charged scalar defined as $H^{\pm}$ with $\tan\beta = \frac{\mathbf{v_2}}{\mathbf{v_1}}$.
- modified gauge couplings,

$$\boxed{y_h^V = g_{SM}^V \times \sin(\beta-\alpha)}\ \boxed{y_H^V = g_{SM}^V \times \cos(\beta-\alpha)}$$

- The Yukawa sector in Type-X 2HDM:

$$-\mathcal{L}_{Yukawa} = Y_{2d}\bar{Q}_L\Phi_2 d_R + Y_{2u}\bar{Q}_L\tilde{\Phi}_2 u_R + Y_{\ell 1}\bar{L}_L\Phi_1 e_R + \text{h.c.} \quad (2)$$

- The factors by which the SM Higgs interaction strengths need to be scaled, are

$$\begin{aligned} y_h^{f_i} &= [\sin(\beta-\alpha) + \cos(\beta-\alpha)\kappa_f]\,, \\ y_H^{f_i} &= [\cos(\beta-\alpha) - \sin(\beta-\alpha)\kappa_f]\,, \\ y_A^{f_i} &= -i\kappa_f \ (\text{for u}), \quad y_A^{f_i} = i\kappa_f \ (\text{for d}, \ \ell), \\ \text{with } \kappa_\ell &\equiv -\tan\beta, \quad \kappa_u = \kappa_d \equiv 1/\tan\beta \end{aligned} \quad (3)$$

- Yukawa couplings here may or may not have the same sign as in the SM case,

- Yukawa couplings here may or may not have the same sign as in the SM case,

$$
\begin{aligned}
y^{f_i}_{h_{SM}} \times y^{V}_{h_{SM}} &> 0 \text{ for SM} - \text{like coupling or right} - \text{sign(RS)}, \\
y^{f_i}_{h_{SM}} \times y^{V}_{h_{SM}} &< 0 \text{ for wrong} - \text{sign(WS)}.
\end{aligned} \tag{4}
$$

- Yukawa couplings here may or may not have the same sign as in the SM case,

$$y^{f_i}_{h_{SM}} \times y^{V}_{h_{SM}} > 0 \text{ for SM}-\text{like coupling or right}-\text{sign(RS)},$$
$$y^{f_i}_{h_{SM}} \times y^{V}_{h_{SM}} < 0 \text{ for wrong}-\text{sign(WS)}. \quad (4)$$

- **Scenario**: $m_h = m_{hSM} = 125 GeV$

Explanation of Muon $(g-2)$

Explanation of Muon $(g-2)$

- The anomalous magnetic moment of muon is an early triumph of quantum field theory and the effect of loop corrections are usually parameterized in terms of $a_\mu = \frac{g_\mu - 2}{2}$.

Explanation of Muon $(g-2)$

- The anomalous magnetic moment of muon is an early triumph of quantum field theory and the effect of loop corrections are usually parameterized in terms of $a_\mu = \frac{g_\mu - 2}{2}$.
- The most recent estimate in SM,

$$a_\mu^{SM} = 116591810(43) \times 10^{-11} \tag{5}$$

Explanation of Muon $(g-2)$

- The anomalous magnetic moment of muon is an early triumph of quantum field theory and the effect of loop corrections are usually parameterized in terms of $a_\mu = \frac{g_\mu - 2}{2}$.
- The most recent estimate in SM,

$$a_\mu^{SM} = 116591810(43) \times 10^{-11} \tag{5}$$

- While the most recent experimental bound by combining the Fermilab data(2021) and earlier BNL(2006),

$$a_\mu^{exp} = 116592040(54) \times 10^{-11} \tag{6}$$

Explanation of Muon $(g-2)$

- The anomalous magnetic moment of muon is an early triumph of quantum field theory and the effect of loop corrections are usually parameterized in terms of $a_\mu = \frac{g_\mu - 2}{2}$.
- The most recent estimate in SM,

$$a_\mu^{SM} = 116591810(43) \times 10^{-11} \tag{5}$$

- While the most recent experimental bound by combining the Fermilab data(2021) and earlier BNL(2006),

$$a_\mu^{exp} = 116592040(54) \times 10^{-11} \tag{6}$$

$$\boxed{\Delta a_\mu = a_\mu^{exp} - a_\mu^{SM} = 251(59) \times 10^{-11}} \tag{7}$$

- There is approximately 4.2σ discrepancy.

- We consider one loop as well as two loop Bar-Zee type contribution to Δa_μ in Type-X 2HDM.

- We consider one loop as well as two loop Bar-Zee type contribution to Δa_μ in Type-X 2HDM.

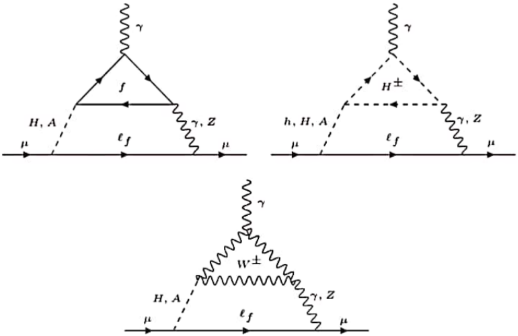

- This kind of diagrams have an enhancement factor of $\frac{M^2}{m_\mu^2}$ over the loop suppression.

- 3σ upper and lower bound on the experimentally observed central value of Δa_μ prefer a region of parameter space on the $m_A - \tan\beta$ plane.

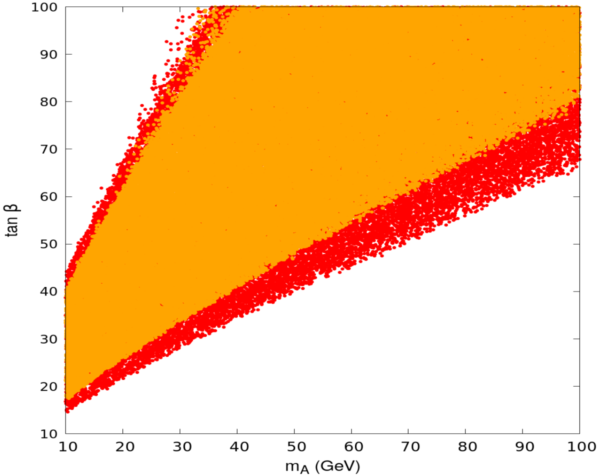

Constraints on model parameters

Constraints on model parameters

- Electroweak precision measurements, restricts $|\Delta m| = |m_{h/H} - m_{H^\pm}|$ depending on m_A and values of $m_{H^\pm}$.

Constraints on model parameters

- Electroweak precision measurements, restricts $|\Delta m| = |m_{h/H} - m_{H^\pm}|$ depending on m_A and values of $m_{H^\pm}$.
- **Theoretical constraints:** include perturbativity, unitarity and vacuum stability conditions at the electroweak scale.

Constraints on model parameters

- Electroweak precision measurements, restricts $|\Delta m| = |m_{h/H} - m_{H^\pm}|$ depending on m_A and values of $m_{H^\pm}$.
- **Theoretical constraints:** include perturbativity, unitarity and vacuum stability conditions at the electroweak scale.
  Vacuum stability:

$$\lambda_{1,2} > 0\,, \tag{8}$$

$$\lambda_3 > -\sqrt{\lambda_1\lambda_2} \tag{9}$$

$$|\lambda_5| < \lambda_3 + \lambda_4 + \sqrt{\lambda_1\lambda_2} \tag{10}$$

$$\lambda_3+\lambda_4-\lambda_5 = \frac{2m_A^2 + y_h^\ell \sin(\beta-\alpha)m_h^2 - (\sin^2(\beta-\alpha) + y_h^\ell \sin(\beta-\alpha))m_H^2}{v^2} \tag{11}$$

- The upper limits on the heavy Higgs masses show quite different behaviors in the RS and WS limit.

$$\lambda_3+\lambda_4-\lambda_5 = \frac{2m_A^2 + y_h^\ell \sin(\beta-\alpha) m_h^2 - (\sin^2(\beta-\alpha) + y_h^\ell \sin(\beta-\alpha)) m_H^2}{v^2} \tag{11}$$

- The upper limits on the heavy Higgs masses show quite different behaviors in the RS and WS limit.
- At large $\tan\beta$ limit, in the right-sign case $(y_h^\ell \sin(\beta-\alpha) \to +1)$ puts a bound,

$$2\frac{m_H^2}{v^2} < \sqrt{0.26 \times 4\pi} + \frac{2m_A^2 + m_h^2}{v^2} \tag{12}$$

$$\lambda_3+\lambda_4-\lambda_5 = \frac{2m_A^2 + y_h^\ell \sin(\beta-\alpha)m_h^2 - (\sin^2(\beta-\alpha) + y_h^\ell \sin(\beta-\alpha))m_H^2}{v^2} \tag{11}$$

- The upper limits on the heavy Higgs masses show quite different behaviors in the RS and WS limit.
- At large $\tan\beta$ limit, in the right-sign case $(y_h^\ell \sin(\beta-\alpha) \to +1)$ puts a bound,

$$2\frac{m_H^2}{v^2} < \sqrt{0.26\times 4\pi} + \frac{2m_A^2 + m_h^2}{v^2} \tag{12}$$

$$\Rightarrow m_H \lesssim 250 \text{ GeV for low } m_A.$$

$$\lambda_3+\lambda_4-\lambda_5 = \frac{2m_A^2 + y_h^\ell \sin(\beta-\alpha)m_h^2 - (\sin^2(\beta-\alpha) + y_h^\ell \sin(\beta-\alpha))m_H^2}{v^2} \quad (11)$$

- The upper limits on the heavy Higgs masses show quite different behaviors in the RS and WS limit.
- At large $\tan\beta$ limit, in the right-sign case $(y_h^\ell \sin(\beta-\alpha) \to +1)$ puts a bound,

$$2\frac{m_H^2}{v^2} < \sqrt{0.26 \times 4\pi} + \frac{2m_A^2 + m_h^2}{v^2} \quad (12)$$

$$\Rightarrow m_H \lesssim 250 \text{ GeV for low } m_A.$$

- In the wrong-sign limit $(y_h^\ell \sin(\beta-\alpha) \to -1)$, m_H can be arbitrarily large.

- **LHC searches** disfavors a large BR($h_{SM} \to AA$)($\lesssim 0.04$).

- **LHC searches** disfavors a large BR($h_{SM} \to AA$)($\lesssim 0.04$).
  1) For our **Scenario,**

$$y_h^\ell \sin(\beta-\alpha) = \frac{g_{hAA}v + m_{12}^2/\sin\beta\cos\beta - 2m_A^2}{m_h^2 - m_H^2} \tag{13}$$

  If we demand perturbativity as well as the condition, $g_{hAA} \approx 0$, then we should get, $y_h^\ell \sin(\beta-\alpha) < 0$.

- **LHC searches** disfavors a large BR($h_{SM} \to AA$)($\lesssim 0.04$).
  1) For our **Scenario,**

$$y_h^\ell \sin(\beta-\alpha) = \frac{g_{hAA} v + m_{12}^2/\sin\beta\cos\beta - 2m_A^2}{m_h^2 - m_H^2} \quad (13)$$

  If we demand perturbativity as well as the condition, $g_{hAA} \approx 0$, then we should get, $y_h^\ell \sin(\beta-\alpha) < 0$.
- Signal strengths of the 125-GeV scalar confine ourselves to the alignment limit ie. $|y_{h/H}^V| \approx 1$ ($y_h^V = \sin(\beta-\alpha)$).

Allowed parameter space

- $m_H, m_H^{\pm} \in [125, 870]$ GeV, $m_A \in [20, 100]$ GeV, $\tan\beta \in [20, 100]$, $|\sin(\beta-\alpha)| \in [0.99, 1]$, $m_{12}^2 \in \left[\frac{m_H^2}{\tan\beta} - 200, \frac{m_H^2}{\tan\beta} + 200\right]$.

Allowed parameter space

- $m_H, m_H^{\pm} \in [125, 870]$ GeV, $m_A \in [20, 100]$ GeV, $\tan\beta \in [20, 100]$, $|\sin(\beta - \alpha)| \in [0.99, 1]$, $m_{12}^2 \in \left[\frac{m_H^2}{\tan\beta} - 200, \frac{m_H^2}{\tan\beta} + 200\right]$.

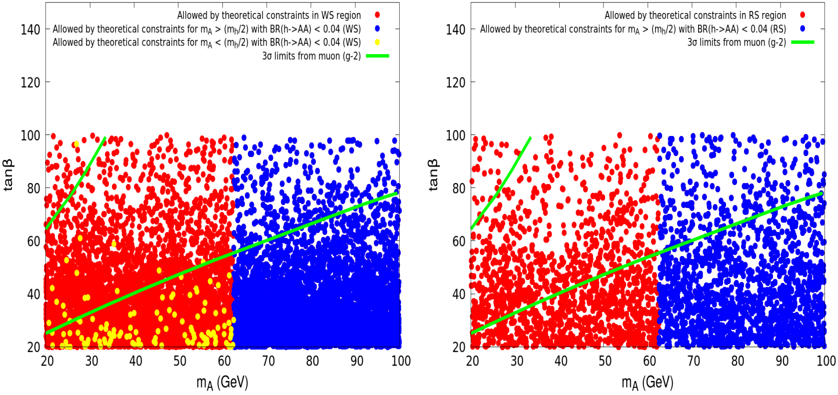

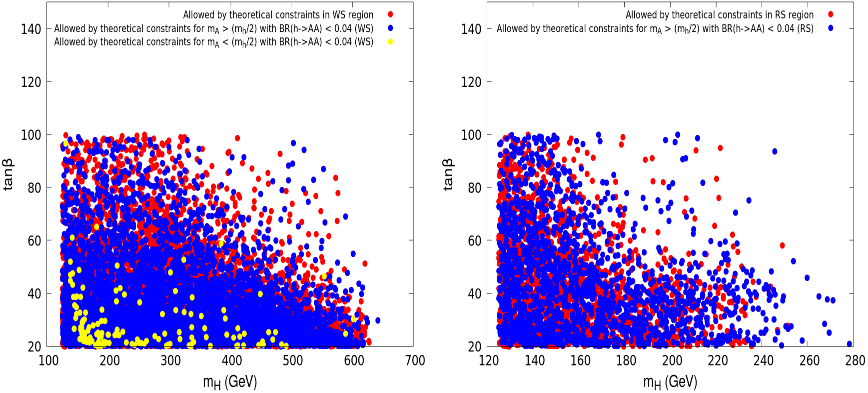
Allowed by theoretical constraints in WS region
Allowed by theoretical constraints for $m_A > (m_h/2)$ with BR(h->AA) < 0.04 (WS)
Allowed by theoretical constraints for $m_A < (m_h/2)$ with BR(h->AA) < 0.04 (WS)
tanβ
m_H (GeV)
Allowed by theoretical constraints in RS region
Allowed by theoretical constraints for $m_A > (m_h/2)$ with BR(h->AA) < 0.04 (RS)
tanβ
m_H (GeV)

Coupling trajectories

- The parameters constrained before are considered at the electroweak scale, set at the pole mass of top quark (~ 173.34 GeV).

Coupling trajectories

- The parameters constrained before are considered at the electroweak scale, set at the pole mass of top quark (~ 173.34 GeV).
- We investigate how they evolve at higher scales and thus obtain their domain of validity in the light of vacuum stability and perturbative unitarity. This yields the cut-off scale $\Lambda_{UV}^{cut-off}$.

	m_H	m_A	$m_{H^\pm}$	λ_1	λ_2	λ_3	λ_4	λ_5
BP1	449.73	80.0	453.89	0.09539	0.25788	6.9130	-3.3549	3.23062
BP2	153.86	63.0	176.15	0.52616	0.25773	0.52559	-0.56774	0.324993

	$\tan\beta$	$\sin(\beta-\alpha)$	$y_h^\ell \times \sin(\beta-\alpha)$
BP1	75.0	0.9996	-1.12095144
BP2	67.0	0.999996	0.81048833

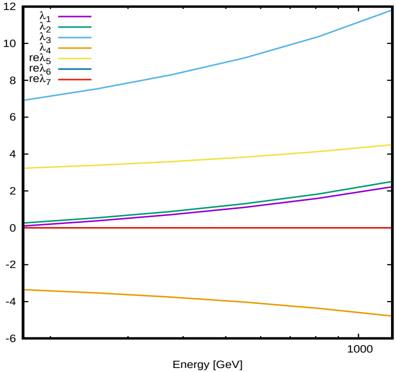

12
10
8
6
4
2
0
-2
-4
-6
1000
Energy [GeV]
λ_1
λ_2
λ_3
λ_4
reλ_5
reλ_6
reλ_7

Figure: BP1

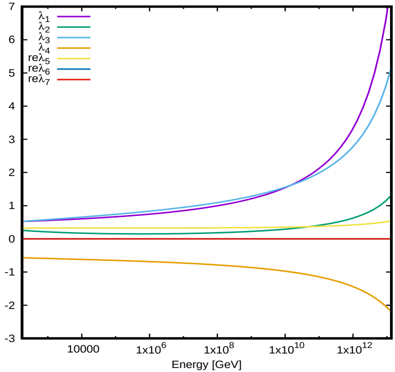
λ1
λ2
λ3
λ4
reλ5
reλ6
reλ7
7
6
5
4
3
2
1
0
-1
-2
-3
10000
1x10^6
1x10^8
1x10^10
1x10^12
Energy [GeV]

Figure: BP2

Allowed regions with various cut-off scales

- We proceed to scan the model parameter space and look for points which satisfy all the theoretical constraints upto cut-off scale $\Lambda_{UV}^{cut-off}(\sim 10^4, 10^8, 10^{16}, 10^{19}$ GeV).

Allowed regions with various cut-off scales

- We proceed to scan the model parameter space and look for points which satisfy all the theoretical constraints upto cut-off scale $\Lambda_{UV}^{cut-off}(\sim 10^4, 10^8, 10^{16}, 10^{19}$ GeV).
- So there are two cases to study,

Allowed regions with various cut-off scales

- We proceed to scan the model parameter space and look for points which satisfy all the theoretical constraints upto cut-off scale $\Lambda_{UV}^{cut-off}(\sim 10^4, 10^8, 10^{16}, 10^{19}$ GeV).
- So there are two cases to study,
  1) Case 1: Scenario with WS Yukawa

Allowed regions with various cut-off scales

- We proceed to scan the model parameter space and look for points which satisfy all the theoretical constraints upto cut-off scale $\Lambda_{UV}^{cut-off}(\sim 10^4, 10^8, 10^{16}, 10^{19}$ GeV).
- So there are two cases to study,
  1) Case 1: Scenario with WS Yukawa
  2) Case 2: Scenario with RS Yukawa

Allowed regions with various cut-off scales

- We proceed to scan the model parameter space and look for points which satisfy all the theoretical constraints upto cut-off scale $\Lambda_{UV}^{cut-off}(\sim 10^4, 10^8, 10^{16}, 10^{19}$ GeV).
- So there are two cases to study,
  1) Case 1: Scenario with WS Yukawa
  2) Case 2: Scenario with RS Yukawa
- We identified the allowed parameter spaces for each of these cases in some two-dimensional planes of relevant physical model parameters.

- **Case 1:**

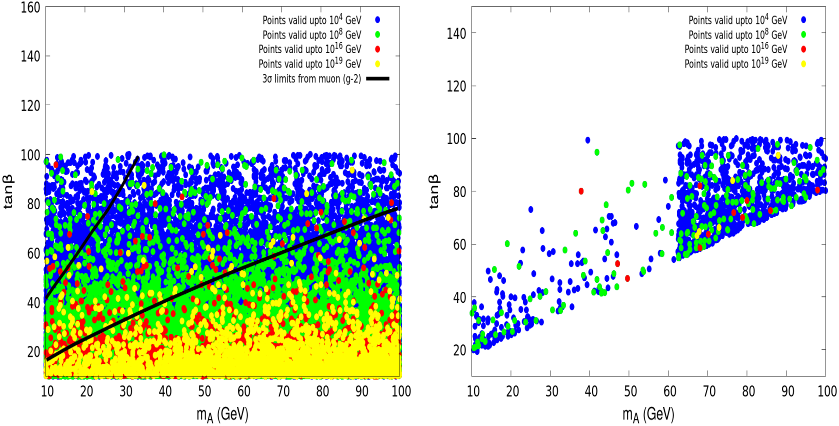
Points valid upto 10^4 GeV
Points valid upto 10^8 GeV
Points valid upto 10^{16} GeV
Points valid upto 10^{19} GeV
3σ limits from muon (g-2)
tanβ
m_A (GeV)
Points valid upto 10^4 GeV
Points valid upto 10^8 GeV
Points valid upto 10^{16} GeV
Points valid upto 10^{19} GeV
tanβ
m_A (GeV)

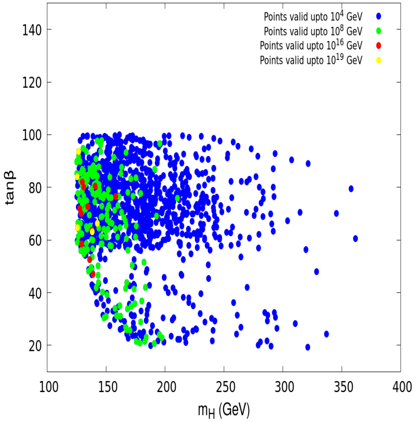
Points valid upto 10^4 GeV
Points valid upto 10^8 GeV
Points valid upto 10^{16} GeV
Points valid upto 10^{19} GeV
tanβ
m_H (GeV)
100
150
200
250
300
350
400
20
40
60
80
100
120
140

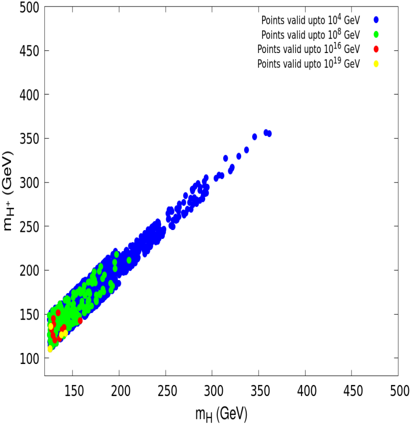
Points valid upto 10^4 GeV
Points valid upto 10^8 GeV
Points valid upto 10^{16} GeV
Points valid upto 10^{19} GeV
m_{H^+} (GeV)
m_H (GeV)
150
200
250
300
350
400
450
500
100
150
200
250
300
350
400
450
500

- **Case 2:**

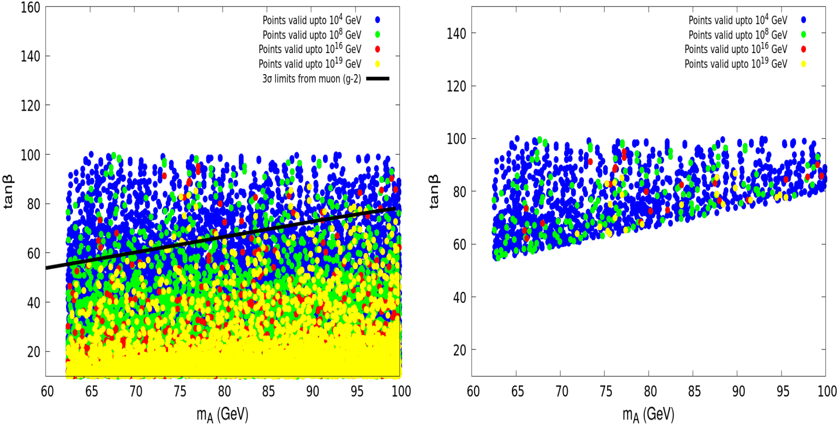

Points valid upto 10^4 GeV
Points valid upto 10^8 GeV
Points valid upto 10^{16} GeV
Points valid upto 10^{19} GeV
3σ limits from muon (g-2)
tanβ
m_A (GeV)
Points valid upto 10^4 GeV
Points valid upto 10^8 GeV
Points valid upto 10^{16} GeV
Points valid upto 10^{19} GeV
tanβ
m_A (GeV)

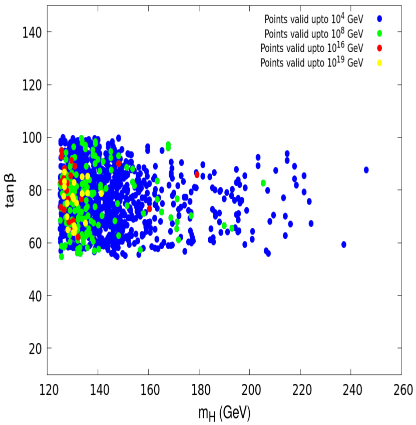
Points valid upto 10^4 GeV
Points valid upto 10^8 GeV
Points valid upto 10^{16} GeV
Points valid upto 10^{19} GeV
tanβ
m_H (GeV)
20
40
60
80
100
120
140
120
140
160
180
200
220
240
260

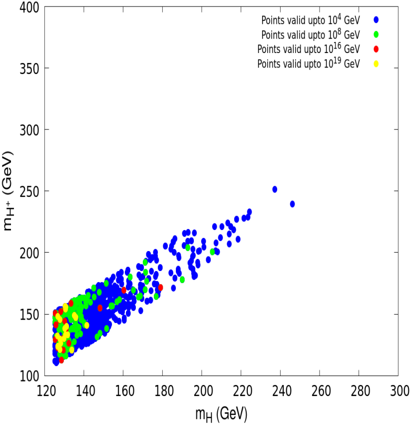
Points valid upto 10^4 GeV
Points valid upto 10^8 GeV
Points valid upto 10^{16} GeV
Points valid upto 10^{19} GeV
m_{H^+} (GeV)
m_H (GeV)
100
150
200
250
300
350
400
120
140
160
180
200
220
240
260
280
300

Conclusion

- We have explored the high-scale validity of Type-X 2HDM, particularly in regions of the parameter space answering to a low-mass neutral CP-odd spinless particle.

Conclusion

- We have explored the high-scale validity of Type-X 2HDM, particularly in regions of the parameter space answering to a low-mass neutral CP-odd spinless particle.
- We have identified the regions in the parameter space, which are helpful in explaining $(g_\mu - 2)$ including the most recent results with other theoretical and experimental constraints.

Conclusion

- We have explored the high-scale validity of Type-X 2HDM, particularly in regions of the parameter space answering to a low-mass neutral CP-odd spinless particle.
- We have identified the regions in the parameter space, which are helpful in explaining $(g_\mu - 2)$ including the most recent results with other theoretical and experimental constraints.
- The two-loop running of various couplings in such regions upto high scales has been studied. thereafter, thus identifying regions where perturbative unitarity and vacuum stability are satisfied upto various high scales, ranging from 10^4 GeV to the Planck scale.

Conclusion

- We have explored the high-scale validity of Type-X 2HDM, particularly in regions of the parameter space answering to a low-mass neutral CP-odd spinless particle.
- We have identified the regions in the parameter space, which are helpful in explaining $(g_\mu - 2)$ including the most recent results with other theoretical and experimental constraints.
- The two-loop running of various couplings in such regions upto high scales has been studied. thereafter, thus identifying regions where perturbative unitarity and vacuum stability are satisfied upto various high scales, ranging from 10^4 GeV to the Planck scale.
- All this bear sample testimony to the Type-X 2HDM being a candidate theory that explains the observed value of $g_\mu - 2$, keeping open a rich set of UV completion possibilities.


Thank you!

Back-up slides: 1

Other diagrams contributing on muon $g-2$:

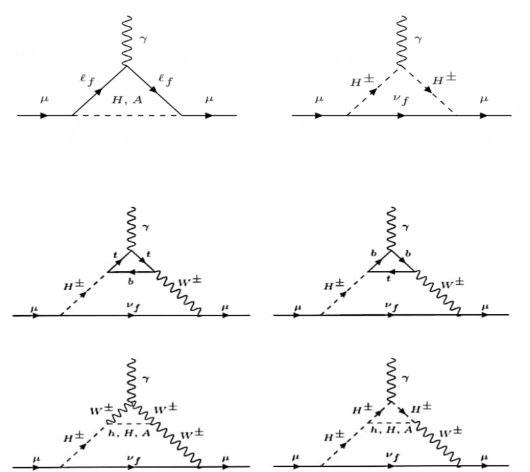

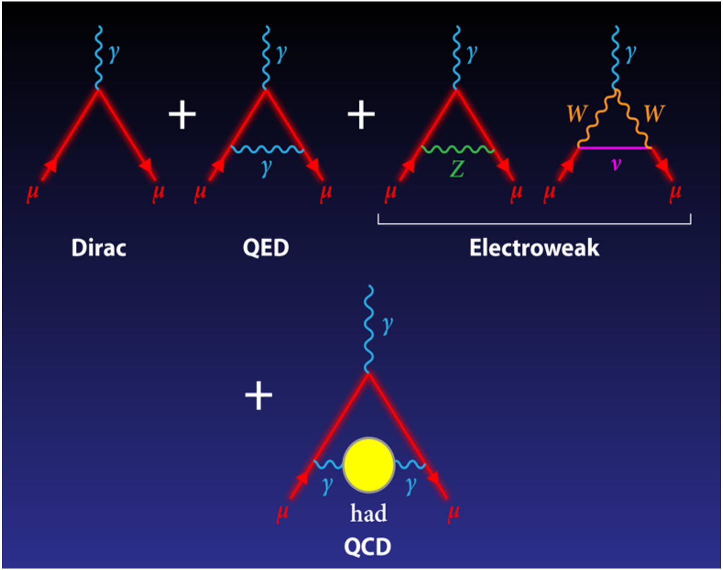
γ
+
μ
Dirac
QED
Z
W
ν
Electroweak
had
QCD

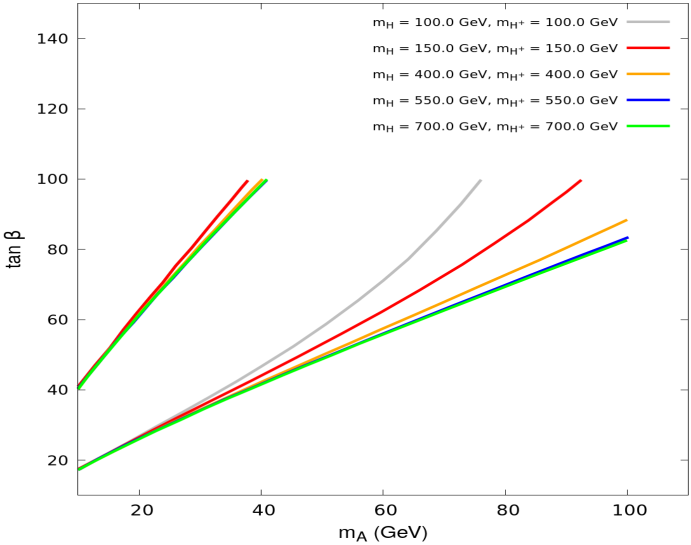

m_H = 100.0 GeV, m_{H^+} = 100.0 GeV
m_H = 150.0 GeV, m_{H^+} = 150.0 GeV
m_H = 400.0 GeV, m_{H^+} = 400.0 GeV
m_H = 550.0 GeV, m_{H^+} = 550.0 GeV
m_H = 700.0 GeV, m_{H^+} = 700.0 GeV
tan β
140
120
100
80
60
40
20
20
40
60
80
100
m_A (GeV)

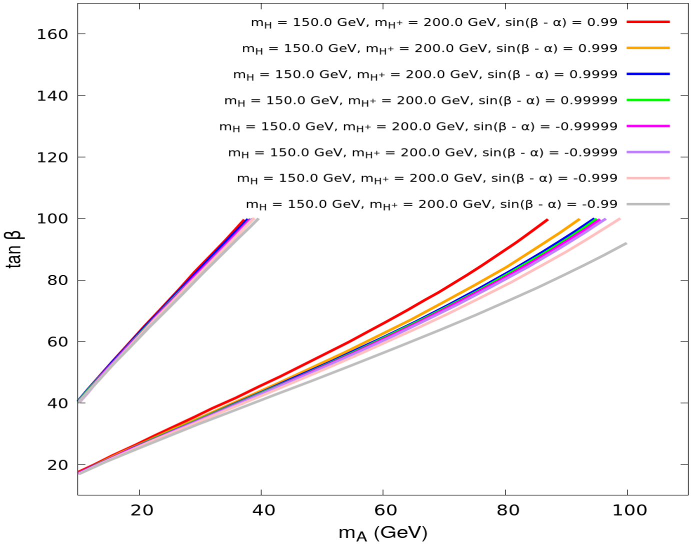
m_H = 150.0 GeV, m_H+ = 200.0 GeV, sin(β - α) = 0.99
m_H = 150.0 GeV, m_H+ = 200.0 GeV, sin(β - α) = 0.999
m_H = 150.0 GeV, m_H+ = 200.0 GeV, sin(β - α) = 0.9999
m_H = 150.0 GeV, m_H+ = 200.0 GeV, sin(β - α) = 0.99999
m_H = 150.0 GeV, m_H+ = 200.0 GeV, sin(β - α) = -0.99999
m_H = 150.0 GeV, m_H+ = 200.0 GeV, sin(β - α) = -0.9999
m_H = 150.0 GeV, m_H+ = 200.0 GeV, sin(β - α) = -0.999
m_H = 150.0 GeV, m_H+ = 200.0 GeV, sin(β - α) = -0.99
tan β
m_A (GeV)
20
40
60
80
100
120
140
160

Back-up slides: 2

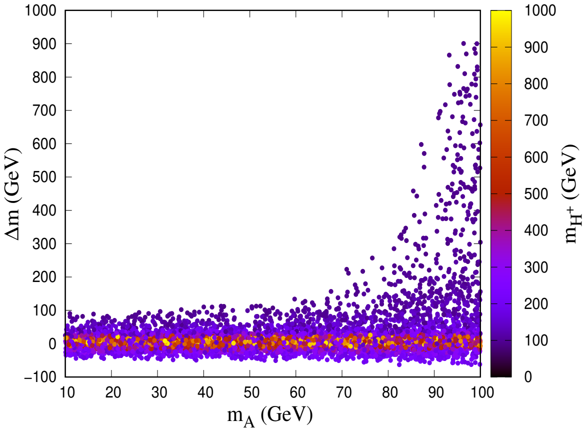

- The physical masses as a function of the quartic couplings:

$$m_A^2 = \frac{m_{12}^2}{\sin\beta\cos\beta} - \lambda_5 v^2 \tag{14}$$

$$m_{H^\pm}^2 \approx m_A^2 + \frac{1}{2}v^2(\lambda_5 - \lambda_4) \tag{15}$$

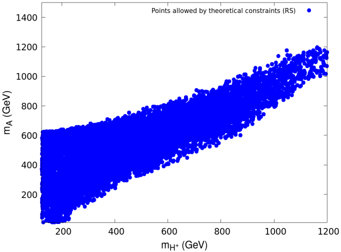

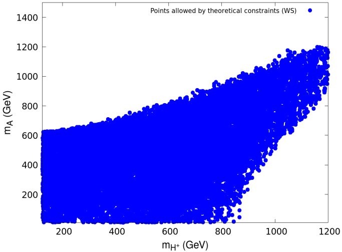

Back-up slides: 3

- the quartic couplings in terms of physical masses and mixing angles.

$$\lambda_1 = \frac{m_H^2 \cos^2\alpha + m_h^2 \sin^2\alpha - m_{12}^2 \tan\beta}{v^2 \cos^2\beta},$$
$$\lambda_2 = \frac{m_H^2 \sin^2\alpha + m_h^2 \cos^2\alpha - m_{12}^2 \cot\beta}{v^2 \sin^2\beta},$$
$$\lambda_3 = \frac{(m_H^2 - m_h^2)\cos\alpha \sin\alpha + 2m_{H^\pm}^2 \sin\beta\cos\beta - m_{12}^2}{v^2 \sin\beta\cos\beta},$$
$$\lambda_4 = \frac{(m_A^2 - 2m_{H^\pm}^2)\sin\beta\cos\beta + m_{12}^2}{v^2 \sin\beta\cos\beta},$$
$$\lambda_5 = \frac{m_{12}^2 - m_A^2 \sin\beta\cos\beta}{v^2 \sin\beta\cos\beta}. \tag{16}$$

Back-up slides: 4

The relevant equations for the running of quartic couplings are given below.

$$16\pi^2\beta^b_{\lambda_1} = \frac{3}{4}g_1^4 + \frac{3}{2}g_1^2 g_2^2 + \frac{9}{4}g_2^4 - 3g_1^2\lambda_1 - 9g_2^2\lambda_1 + 12\lambda_1^2 + 4\lambda_3^2 + 4\lambda_3\lambda_4 + 2\lambda_4^2 + 2\lambda_5^2$$

$$16\pi^2\beta^Y_{\lambda_1} = -4Y_\tau^4 + 4Y_\tau^2\lambda_1$$

$$16\pi^2\beta^b_{\lambda_2} = \frac{3}{4}g_1^4 + \frac{3}{2}g_1^2 g_2^2 + \frac{9}{4}g_2^4 - 3g_1^2\lambda_2 - 9g_2^2\lambda_2 + 12\lambda_2^2 + 4\lambda_3^2 + 4\lambda_3\lambda_4 + 2\lambda_4^2 + 2\lambda_5^2$$

$$16\pi^2\beta^Y_{\lambda_2} = -12Y_b^4 - 12Y_t^4 + \left(12Y_b^2 + 12Y_t^2\right)\lambda_2$$

$$
\begin{aligned}
16\pi^2\beta^b_{\lambda_3} =& \frac{3}{4}g_1^4 - \frac{3}{2}g_1^2 g_2^2 + \frac{9}{4}g_2^4 - 3g_1^2\lambda_3 - 9g_2^2\lambda_3 \\
&+ (\lambda_1+\lambda_2)(6\lambda_3+2\lambda_4) + 4\lambda_3^2 + 2\lambda_4^2 + 2\lambda_5^2 \\
16\pi^2\beta^Y_{\lambda_3} =& \left(6Y_b^2 + 6Y_t^2 + 2Y_\tau^2\right)\lambda_3 \\
16\pi^2\beta^b_{\lambda_4} =& 3g_1^2 g_2^2 - \left(3g_1^2 + 9g_2^2\right)\lambda_4 + 2\lambda_1\lambda_4 + 2\lambda_2\lambda_4 + 8\lambda_3\lambda_4 + 4\lambda_4^2 + 8\lambda_5^2 \\
16\pi^2\beta^Y_{\lambda_4} =& \left(6Y_b^2 + 6Y_t^2 + 2Y_\tau^2\right)\lambda_4 \\
16\pi^2\beta^b_{\lambda_5} =& \left(-3g_1^2 - 9g_2^2 + 2\lambda_1 + 2\lambda_2 + 8\lambda_3 + 12\lambda_4\right)\lambda_5 \\
16\pi^2\beta^Y_{\lambda_5} =& \left(6Y_b^2 + 6Y_t^2 + 2Y_\tau^2\right)\lambda_5 \qquad (17)
\end{aligned}
$$

Back-up slides: 5

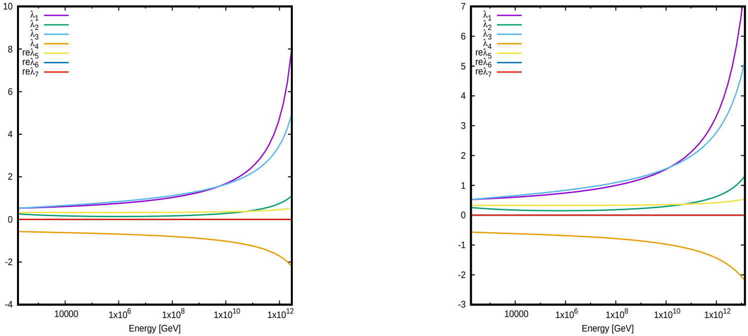

Figure: One-loop(left) and two-loop(right) RG running of quartic couplings for BP3.

Back-up slides: 6

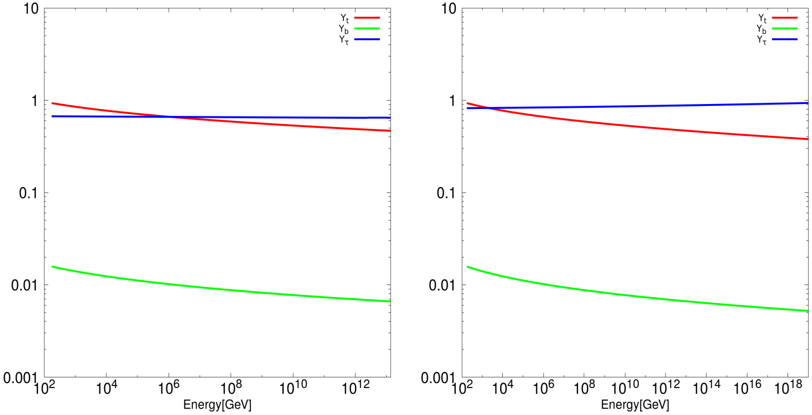

Figure: *Two-loop RG running of third generation Yukawa couplings.*

Back-up slides: 7

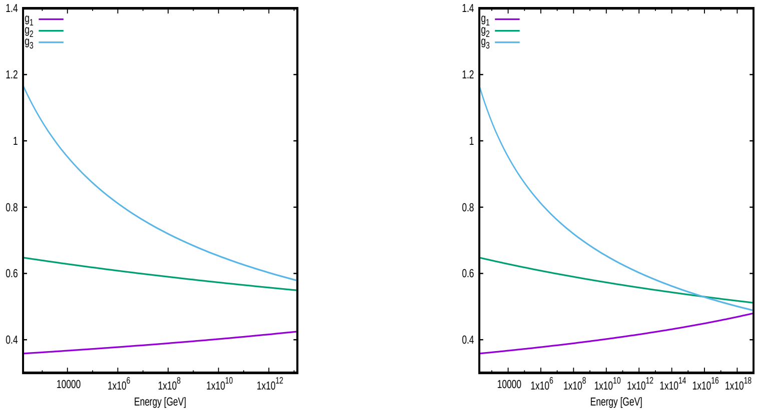

Figure: *Two-loop RG running of gauge couplings.*